LETTERS

A mutation in *Ihh* that causes digit abnormalities alters its signalling capacity and range

Bo Gao[1,2]*, Jianxin Hu[1,2]*, Sigmar Stricker[3,4], Martin Cheung[1,5], Gang Ma[2], Kit Fong Law[1], Florian Witte[3,4,6], James Briscoe[7], Stefan Mundlos[3,4], Lin He[2,8,9], Kathryn S. E. Cheah[1,5] & Danny Chan[1,5]

Brachydactyly type A1 (BDA1) was the first recorded disorder of the autosomal dominant Mendelian trait in humans, characterized by shortened or absent middle phalanges in digits. It is associated with heterozygous missense mutations in indian hedgehog (*IHH*)[1,2]. Hedgehog proteins are important morphogens for a wide range of developmental processes[3,4]. The capacity and range of signalling is thought to be regulated by its interaction with the receptor PTCH1 and antagonist HIP1. Here we show that a BDA1 mutation (E95K) in *Ihh* impairs the interaction of IHH with PTCH1 and HIP1. This is consistent with a recent paper showing that BDA1 mutations cluster in a calcium-binding site essential for the interaction with its receptor and cell-surface partners[5]. Furthermore, we show that in a mouse model that recapitulates the E95K mutation, there is a change in the potency and range of signalling. The mice have digit abnormalities consistent with the human disorder.

Mutations in human *SHH* and *IHH* cause developmental defects such as holoprosencephaly[6], acrocapitofemoral dysplasia[7] and BDA1 (refs 1, 2). However, the molecular basis of these mutations is not known. To investigate the mechanism underlying BDA1 *in vivo*, we generated mice with the Ihh^{E95K} mutation by gene targeting (Supplementary Fig. 1). $Ihh^{+/E95K}$ mice showed shortened middle phalanges in digits II and V, indicating a dominant effect of the mutation on digit formation, because mice heterozygous for an *Ihh* null mutation have normal digits (Fig. 1a and Supplementary Fig. 2a). Homozygous mice ($Ihh^{E95K/E95K}$) showed a classic BDA1 phenotype with severely shortened (II–IV) or absent middle phalanges (digit V), and abnormal and shortened limb skeletal elements from embryonic day (E)13.5 (Supplementary Fig. 2b–d). Because heterozygous mutants are only mildly affected, subsequent analyses were performed on homozygous mutants, referred to as BDA1 mice.

In limb development, SHH acts early, regulating patterning and growth[8]. IHH acts later and is thought not to affect patterning, but to regulate endochondral bone formation by controlling chondrogenic differentiation and proliferation[9]. The mammalian growth plate is an ideal system to study IHH signalling because it is organized into distinct zones that progress from round chondrocytes to flattened proliferating cells organized into columns, to larger non-dividing prehypertrophic cells that express *Ihh*, and finally to even larger hypertrophic chondrocytes expressing *Col10a1* (ref. 9). Endochondral ossification in the mutants was retarded, as indicated by the delayed expression of *Ihh* and *Col10a1* in the developing ulna and radius of heterozygous and homozygous mice at E14.5 (Supplementary Fig. 2e). The range and capacity of IHH signalling can be monitored by the expression of hedgehog targets *Ptch1* and *Gli1*. In wild-type mice at E15.5, the expression of *Ptch1* (Fig. 1b and Supplementary Fig. 3) and *Gli1* (data not shown) decreased gradually from the source of IHH (prehypertrophic chondrocytes) to the proliferative zone. In BDA1 mice, *Ptch1* expression in the proliferating zone was initially reduced and the gradient faded more quickly across the proliferative zone than in wild-type mice, indicating a change in the IHH activity gradient. IHH promotes chondrocyte proliferation in the growth plate[10]. Pulse-labelling with BrdU at E15.5 revealed fewer BrdU-positive chondrocytes in the developing cartilage anlagen of the limb bones in BDA1 mice (Fig. 1c, d), consistent with a reduced capacity of IHH to stimulate chondrocyte proliferation. Quantification of the IHH–PTCH1 binding affinity using a cell-based assay[11] showed a higher dissociation constant (K_d) for IHH(E95K) (40.6 nM) than IHH (20.6 nM), indicating a markedly reduced binding affinity of IHH(E95K) (Fig. 1e) that could explain the reduced signalling capacity. Furthermore, analysis from an *in vitro* cell assay showed that the signalling capacity of IHH(E95K) was reduced to about 70% of wild type (Supplementary Fig. 4).

In the growth plate, there is also a 'long-range' IHH signal to the periarticular region where it activates the expression of *PthrP* (also known as *Pthlh*) as part of the IHH–PTHrP negative feedback regulatory loop[10,12]. Notably, in BDA1 mice, despite the reduced 'short-range' hedgehog signalling, periarticular expression of *Ptch1* (Fig. 1b) and *PthrP* (Supplementary Fig. 3a) was increased, indicating that IHH(E95K) had travelled further than normal. CDO (also known as CDON) is a positive regulator of hedgehog signalling[13], whereas PTCH1 and HIP1 are negative regulators[14]. Hedgehog induces expression of *Ptch1* and *Hip1* to form a feedback loop that restricts hedgehog signalling[4]. A plausible explanation for the altered signalling in BDA1 mice is that an impaired interaction with PTCH1 and other signal transducers decreases the signalling efficacy of IHH but also decreases its retention close to its source allowing it to diffuse further. An alternative is that the mutation affects the multimerization and stability of IHH. However, this is not known and we favour the former because the signalling capacity of IHH(E95K) is reduced in C3H10T1/2 cells (Supplementary Fig. 4), and BDA1 missense mutations in IHH affect its interactions with PTCH1, HIP and CDO[5].

We studied further the affect of the E95K mutation on digit development. In the developing digit, *Hip1* is expressed at the periphery of the condensed cartilage elements, as well as in the proximal and distal margins of adjacent cartilage elements flanking the interzone—the site

[1]Department of Biochemistry, the University of Hong Kong, Hong Kong, China. [2]Bio-X Center, Shanghai Jiao Tong University, 1954 Huashan Road, Shanghai 200030, China. [3]Max-Planck Institute for Molecular Genetics, Ihnestrasse 73, 14195 Berlin, Germany. [4]Institut für Medizinische Genetik, Charité, Universitätsmedizin Berlin, Augustenburger Platz 1, 13353 Berlin, Germany. [5]Centre for Reproduction, Development and Growth, LKS Faculty of Medicine, The University of Hong Kong, Pokfulam, Hong Kong, China. [6]Institute for Chemistry/Biochemistry, Free University Berlin, Thielallee 63, 14195 Berlin, Germany. [7]Developmental Neurobiology, National Institute for Medical Research, Mill Hill, London NW7 1AA, UK. [8]Institute for Nutritional Sciences, Shanghai Institutes of Biological Sciences, Chinese Academy of Sciences, Shanghai 200031, China. [9]Institutes of Biomedical Sciences, Fudan University, Shanghai 200032, China.
*These authors contributed equally to this work.

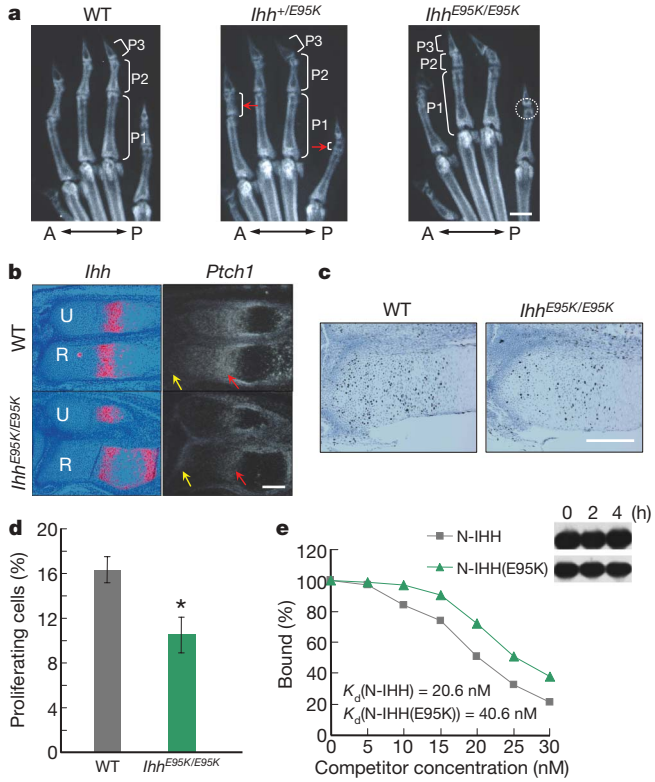

Figure 1 | E95K mutation in IHH altered the capacity and range of hedgehog signalling in BDA1 mouse. **a**, Digit radiography of 7-weeks-postnatal mice. Digits I–V are numbered from anterior (A) to posterior (P). The middle phalanges of digits II and V were shortened in $Ihh^{+/E95K}$ mice (red arrow). In $Ihh^{E95K/E95K}$ mice, the middle phalanges were all shortened in digits II–IV and missing in digit V (dotted circle). P1, proximal phalange; P2, middle phalange; P3, distal phalange; WT, wild type. **b**, In the wild type, *Ptch1* expression relative to the *Ihh* expression domain showed a gradient with a gradual decrease from the IHH source. In contrast, *Ptch1* expression decreased markedly from the IHH source in the $Ihh^{E95K/E95K}$ mouse growth plate (red arrow regions), but was maintained/increased in the periarticular region (yellow arrow regions). R, radius; U, ulna. **c**, Mice at E15.5 were labelled with BrdU for 2 h; labelled cells were detected using an anti-BrdU antibody in consecutive sections. **d**, Quantitative analysis of the labelled cells in **c**. The percentage of proliferating cells was significantly reduced in $Ihh^{E95K/E95K}$ compared to wild-type mice ($n = 3$; $^*P = 0.036$, Student's *t*-test). Error bars are s.d. **e**, Interaction of the amino-terminal fragments of IHH (N-IHH) and IHH(E95K) (N-IHH(E95K)) with PTCH1. The binding affinity was determined using a cell-based competition assay for the binding of ^{32}P-labelled N-IHH protein to cells expressing PTCH1 (ref. 11), with an increasing concentration of unlabelled N-IHH or N-IHH(E95K). The K_d for PTCH1 determined from the competition graphs showed a clear difference between N-IHH and N-IHH(E95K) as indicated. The gel insert shows a stability test of the purified N-IHH and N-IHH(E95K) proteins under conditions of the binding assay assessed by western blot, indicating that there was no notable degradation of N-IHH or N-IHH(E95K) within the assay period. Scale bars, 1 mm (**a**) and 200 μm (**b**, **c**).

of the future joint (Fig. 2a). Thus, HIP1 in the developing digit could assist other hedgehog partners in maintaining IHH signalling within range of the cartilage anlagen. *Ihh* is initially expressed in the centre of the condensing mesenchyme of the cartilage elements that flank the interzone regions from E13.5. Morphologically, these *Ihh*-expressing cells are no different from the surrounding cells (data not shown). The function of *Ihh* expression at this stage of digit development has not been well studied, but *Ptch1* and *Gli1* (Fig. 2a and Supplementary Fig. 5) expression patterns clearly indicate IHH activity throughout the condensing mesenchyme. IHH signalling is less intense in the interzone regions, where *Gdf5* is expressed (Fig. 2a). In the developing digits of BDA1 mice, there seemed to be a general decrease in IHH activity but, as in the growth plate, it extended further from the source than in

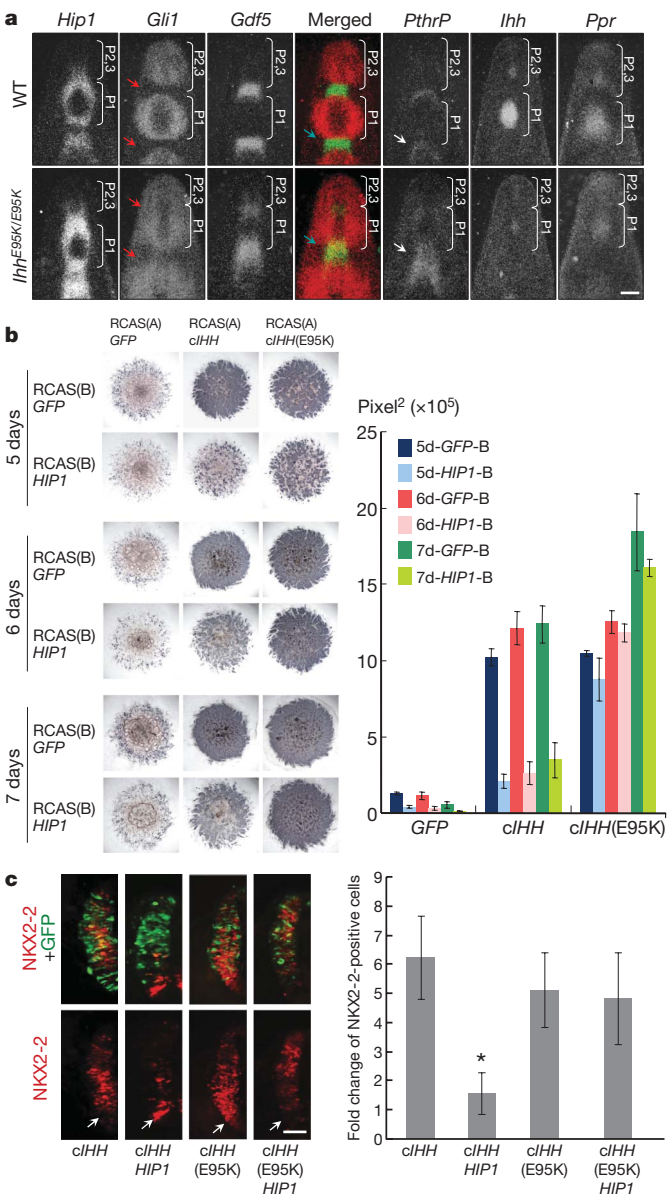

Figure 2 | IHH signals into the interzone in the developing digit of BDA1 mice owing to impaired interaction with HIP1. **a**, Molecular analysis of digit formation at E13.5. Expression of *Hip1*, *Gli1*, *Gdf5*, *PthrP*, *Ihh* and *Ppr* (also known as *Pth1r*) using radioactive *in situ* hybridization on sagittal sections of digit III. *Hip1* was expressed at the margin demarcating the cartilage element. *Gli1* (red) and *Gdf5* (green) expression signals from consecutive sections are merged, showing increased hedgehog signalling in the developing interzone (yellow; blue arrow region). Diffused *Gli1* expression was noted (red arrows), indicating wider spread of the hedgehog signal, and concomitant with an expanded interzone indicated by *Gdf5* expression. Increased *PthrP* expression in the developing interzone was also noted (white arrows). *Ppr* was expressed in the same domains as *Ihh*. P1, proximal phalange; P2, middle phalange; P3, distal phalange. **b**, Micromass cultures infected with RCAS(A) constructs and co-infected with RCAS(B) constructs carrying either *GFP* (control) or *HIP1*. Representative cultures stained for alkaline phosphatase (ALP) activity at indicated times are shown on the left; quantification of the stained surface area using the morphometric tool AutMess is shown on the right ($n = 4$). Chicken *IHH* and *IHH*(E95K) robustly induce ALP activity. Co-infection of RCAS(B)*HIP1* markedly reduces ALP induction by c*IHH*, but only mildly inhibits ALP induction by c*IHH*(E95K). **c**, Induction of NKX2-2 in response to overexpression of c*IHH* or c*IHH*(E95K) in the presence or absence of *HIP1* in the developing chick neural tube. The arrows indicate region of the endogenous vp3 progenitor cells. The NKX2-2-expressing cells were counted (three sections per neural tube, $n = 5$), and the fold change in NKX2-2-positive cells relative to a control GFP electroporation is shown. $^*P < 0.0001$, Student's *t*-test. Scale bars, 100 μm (**a**) and 50 μm (**c**); error bars are s.d.

wild-type mice, overlapping with the *Gdf5*-expressing domain of the interzone (Fig. 2a). This signalling pattern is in keeping with an increased movement of IHH(E95K) owing to impaired interaction with HIP1 and other partners. Consistent with an increased IHH signalling range, *Hip1*, *Gli1* and *PthrP* expression were increased in the interzone (Fig. 2a).

BDA1 mutations in IHH affect its binding to HIP[5]. We tested the consequence of the E95K mutation on hedgehog signalling using a chick limb bud micromass culture assay[15]. Overexpression of IHH impaired the chondrogenic differentiation of limb bud mesenchymal cells, instead promoting differentiation to cells expressing alkaline phosphatase (Fig. 2b). This effect of IHH was suppressed in the presence of HIP1, supporting HIP1 as a negative regulator of IHH signalling (Fig. 2b). IHH(E95K) similarly promoted differentiation, but this effect was not suppressed in the presence of HIP1 (Fig. 2b). Thus, the regulation of hedgehog signalling by HIP1 is impaired by the E95K mutation. A similar finding was observed when chondrogenesis was used as readout (Supplementary Fig. 6). We studied this further using *in ovo* electroporation to introduce IHH or IHH(E95K) into the developing chick neural tube[16]. In response to the endogenous SHH signal from the notochord and floor plate, *NKX2-2* is normally activated in ventral progenitor cells closest to the SHH source[17]. Forced expression of chicken IHH (cIHH) resulted in non-cell autonomous activation of NKX2-2 in the electroporated region of the neural tube (Fig. 2c). This inducing activity was markedly reduced when HIP1 was co-expressed with IHH (Fig. 2c). Overexpression of cIHH(E95K) also induced NKX2-2, however, this effect was not inhibited by coexpression of HIP1. This is consistent with the *in vitro* finding.

Thus, in the growth plate, the impaired interaction of IHH(E95K) with its receptor PTCH1 may reduce the immediate signalling capacity of IHH emanating from the prehypertrophic chondrocytes. Reduced binding to PTCH1 and other partners such as HIP1 would allow IHH(E95K) to travel further, increasing its stimulation of *PthrP* transcription at the perichondrium. Together, these abnormalities cause reduced bone growth in the BDA1 mouse. Fine-tuning of the IHH signal may be important for regulating bone growth; indeed, recent genome-wide genetic association studies in two large populations of loci that influence adult height identified genes in the hedgehog signalling pathway, including *IHH*, *HIP1* and *PTCH1* (refs 18, 19).

For the digits, we propose that the enhanced signalling range of IHH(E95K) in BDA1 mouse is the primary stimulus underlying the defect. This is supported by findings that activation of hedgehog signalling in chondrocytes by conditional ablation of *Ptch1* leads to joint defects[20]. In heterozygous *short digit* mice, an inversion in the *Shh* locus ectopically activates *Shh* in the developing phalanges in the proximal digital elements, resulting in increased *PthrP* in the interzone region, loss or reduced *Ihh* expression in distal digit elements, and mis-expression of *Gdf5*; a combination that results in a BDA1 phenotype[21].

A question remains as to how the shortened or missing middle phalanges can be explained in the BDA1 mouse model. Measurement of the most distal cartilage element before the last joint that is formed showed this element to be markedly shorter in the BDA1 mouse (Fig. 3a). Using pulse-chase labelling with BrdU, we showed that in wild-type mice, proximodistal outgrowth involves the recruitment of surrounding proliferating mesenchymal cells into the condensing distal cartilage digit element (Fig. 3b), and that this process is reduced in the BDA1 mouse to about 40% of normal (Fig. 3c, d). Although FGF signalling from the apical ectodermal ridge is thought to be important in regulating the size of the cartilage elements, which can influence the location and number of phalangeal segmentations[22], *Fgf8* expression was normal in BDA1 mice (Supplementary Fig. 7), suggesting that IHH may have a more direct role. Indeed, we showed intense *Gli1* expression at the distal tip of wild-type mice from E13.5, which was reduced in the BDA1 mouse (Fig. 3e), consistent with reduced *Ihh* expression in the most distal cartilage element in the BDA1 mouse (Fig. 3f). Therefore, in addition

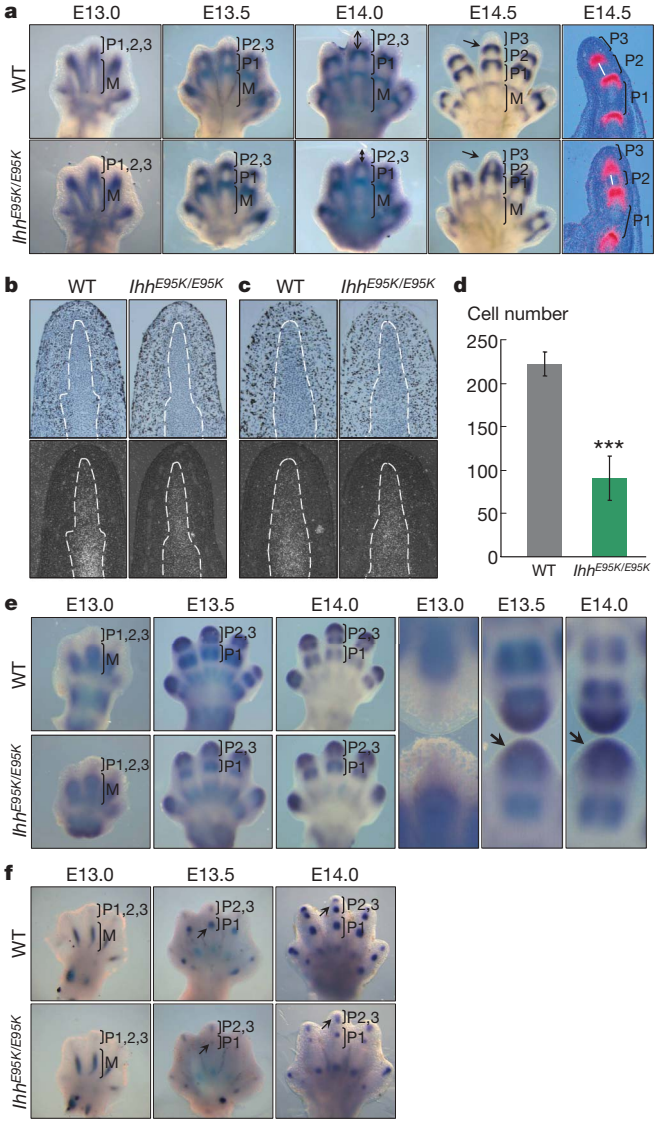

Figure 3 | Impaired digit outgrowth in BDA1 mouse from reduced IHH signalling at the distal tip. **a**, *Gdf5* expression in the developing digits of the hind limb from E13.0 to E14.5. Cartilage elements in digit III (M, metatarsal; P1, proximal phalange; P2, middle phalange; P3, distal phalange) showed no notable developmental difference between wild-type (WT) and $Ihh^{E95K/E95K}$ mice at E13.0. From E13.5, a slight reduction in distal digit outgrowth was noted that became obvious by E14.0 (regions marked by double-arrow lines), with shortened P2 and P3 elements at E14.5. Radioactive *in situ* hybridization of sagittal sections for digit III at E14.5 highlights the shortened middle phalangeal element (white lines). **b**, Two-hour pulse-labelling with BrdU. BrdU staining showed proliferating mesenchymal cells surrounding the chondrogenic condensation (regions enclosed by white dotted lines) delineated by the expression of *Col2a1* in a consecutive section (shown below the corresponding sections). No difference was found between wild-type and $Ihh^{E95K/E95K}$ mice. **c**, Two-hour pulse/10-h chase-labelling with BrdU. After a 10-h chase, BrdU-positive cells were detected within the distal *Col2a1* expression domain, which is fewer in $Ihh^{E95K/E95K}$ than wild-type mice, indicating impaired recruitment at the distal tip region. **d**, Quantitative analysis of BrdU-positive cells showing a significant decrease in $Ihh^{E95K/E95K}$ mice ($n = 5$; error bars indicate s.d.; $^{***}P < 0.0001$, Student's *t*-test). **e**, Whole-mount *in situ* hybridization for the expression of *Gli1* in hind limb digits from E13.0 to E14.0, showing reduced expression at the tip region in $Ihh^{E95K/E95K}$ mice. To demonstrate the reduction, digits III of the wild-type and $Ihh^{E95K/E95K}$ mice are compared tip-to-tip with higher magnification in panels to the right (black arrow regions). **f**, Expression of *Ihh* in digit cartilage elements of $Ihh^{E95K/E95K}$ mice was similar to wild-type at E13.0, but reduced at E13.5 and E14.0 (black arrow). The separation of P2 and P3 *Ihh* expression domains was delayed in $Ihh^{E95K/E95K}$ mice at E14.0.

to FGF, IHH signal from the condensed mesenchyme is also important for proper distal digit outgrowth. Recently, SHH was shown to function in a growth-promoting phase in the recruitment of digit precursor mesenchyme before E13.0 (ref. 8). Our data indicate IHH functions similarly, but acts later (after E13.0) in the outgrowth of distal phalangeal elements.

Our findings provide, to our knowledge, the first insight into the *in vivo* consequence of hedgehog mutations that impair interaction with hedgehog partners, and strongly implicate altered IHH signalling capacity and range in the pathogenesis of BDA1 (Fig. 4a). Our model for enhanced long-range signalling is consistent with a theoretical model in which an increase in the effective diffusion coefficient, such as that caused by reducing retention on binding proteins, lowers the responses close to the source but increases those at a distance[23]. We propose a mechanism for the digit abnormality in BDA1 (Fig. 4b, c) in which reduced IHH signalling at the digit tip region results in shortened cartilage elements that are either too short for the last joint to be formed (digit V in the BDA1 mouse), or form a joint with severely shortened middle phalanges (digits II–IV in the BDA1 mouse). In mice, this phenotype is most prominent in the homozygous state, whereas BDA1 is dominant in humans. The reason for this is not known but it is not uncommon[24,25], and it may be related to modifying genes and the variations in the capacity of a signalling molecule to induce an effect between mouse and human.

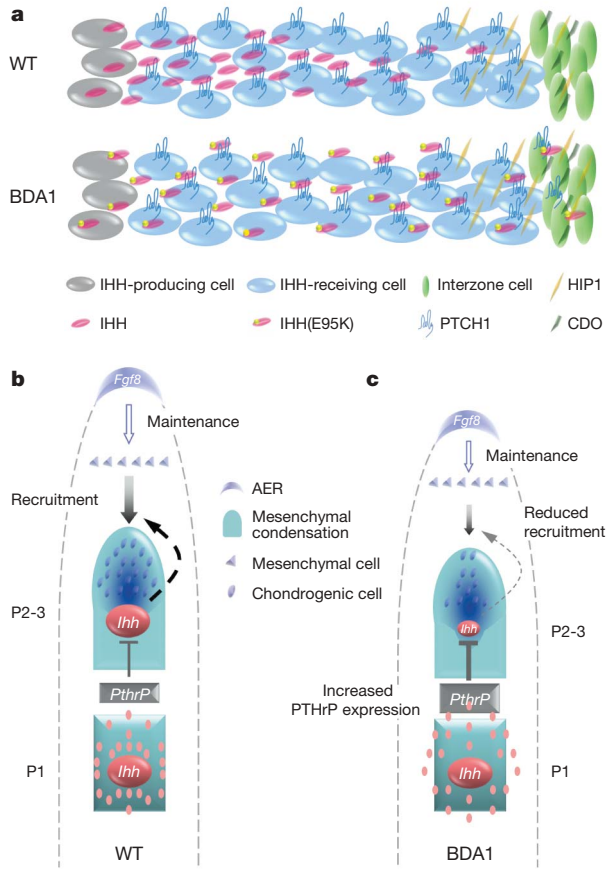

Figure 4 | Model for the molecular mechanism of the E95K mutation altering IHH signalling causing BDA1. a, Model illustrating the normal range of IHH signalling in the developing digit in which interaction with PTCH1 and HIP1 retains the signal within the cartilage element. In the BDA1 mouse the interaction with PTCH1 and HIP1 is weakened, allowing the IHH(E95K) to diffuse further into the interzone region. **b**, The proposed role of IHH during early digit patterning and its regulation. *Ihh* expressed in the distal phalangeal condensation signals to the undifferentiated proliferating mesenchymal cells under the apical ectodermal ridge and promotes recruitment/chondrogenesis for digit outgrowth in conjunction with FGF signalling. We propose that *Ihh* expression in the distal elements is regulated by signals mediated in the proximal interzone, probably PTHrP as *Ppr* is expressed in the *Ihh* domain, through the negative feedback loop modulating chondrocyte differentiation. **c**, In BDA1 mice, the range of IHH signal is increased in the proximal element, extending further into the developing interzone region, upregulating genes such as *PthrP*. This increases its signal to the distal condensed mesenchyme where *Ppr* is expressed and downregulates *Ihh* expression, reducing recruitment/chondrogenesis and thereby the size of the distal element. Thus, P2–P3 segmentation begins within a smaller chondrogenic template, resulting in a smaller template for the future middle phalange (P2). P1, proximal phalange.

METHODS SUMMARY

Embryonic stem cells carrying the E95K mutation were generated by homologous recombination. These cells were used to produce mouse chimaeras that were crossed with β-actin *Cre* mice[26] to remove the neomycin (*neo*) cassette in conjunction with germline transmission of the targeted allele. Mice of 129SvEv or mixed 129SvEv-ICR backgrounds were used as there were no differences in the phenotypic outcome. X-rays were taken using a General Electric X-ray machine (Senograph 600T Senix HF, General Electric). Skeletal preparations were stained with Alizarin Red S and Alcian Blue[27]. Pulse-chase labelling with BrdU was performed by injection of thymidine to dilute BrdU incorporation during the chase period[28]. *In situ* hybridization and immunostaining were performed on 5-μm dewaxed sections using [^{35}S]-UTP-labelled riboprobes[29]. *IHH* and *IHH^{E95K}*, and *HIP1* were overexpressed in chick limb bud micromass cultures using the RCAS(A) and RCAS(B) viruses, respectively[15]. These genes were also overexpressed in the developing chick neural tube by electroporation of the respective expression constructs[16].

Full Methods and any associated references are available in the online version of the paper at www.nature.com/nature.

Received 1 July 2008; accepted 12 February 2009.
Published online 1 March 2009.

1. Gao, B. *et al.* Mutations in *IHH*, encoding Indian hedgehog, cause brachydactyly type A–1. *Nature Genet.* **28,** 386–388 (2001).
2. McCready, M. E., Grimsey, A., Styer, T., Nikkel, S. M. & Bulman, D. E. A century later Farabee has his mutation. *Hum. Genet.* **117,** 285–287 (2005).
3. Hooper, J. E. & Scott, M. P. Communicating with Hedgehogs. *Nature Rev. Mol. Cell Biol.* **6,** 306–317 (2005).
4. Jiang, J. & Hui, C. C. Hedgehog signaling in development and cancer. *Dev. Cell* **15,** 801–812 (2008).
5. McLellan, J. S. *et al.* The mode of Hedgehog binding to Ihog homologues is not conserved across different phyla. *Nature* **455,** 979–983 (2008).
6. Wallis, D. & Muenke, M. Mutations in holoprosencephaly. *Hum. Mutat.* **16,** 99–108 (2000).
7. Hellemans, J. *et al.* Homozygous mutations in *IHH* cause acrocapitofemoral dysplasia, an autosomal recessive disorder with cone-shaped epiphyses in hands and hips. *Am. J. Hum. Genet.* **72,** 1040–1046 (2003).
8. Zhu, J. *et al.* Uncoupling Sonic hedgehog control of pattern and expansion of the developing limb bud. *Dev. Cell* **14,** 624–632 (2008).
9. Kronenberg, H. M. Developmental regulation of the growth plate. *Nature* **423,** 332–336 (2003).
10. St-Jacques, B., Hammerschmidt, M. & McMahon, A. P. Indian hedgehog signaling regulates proliferation and differentiation of chondrocytes and is essential for bone formation. *Genes Dev.* **13,** 2072–2086 (1999); erratum **13,** 2617 (1999).
11. Fuse, N. *et al.* Sonic hedgehog protein signals not as a hydrolytic enzyme but as an apparent ligand for patched. *Proc. Natl Acad. Sci. USA* **96,** 10992–10999 (1999).
12. Vortkamp, A. *et al.* Regulation of rate of cartilage differentiation by Indian hedgehog and PTH-related protein. *Science* **273,** 613–622 (1996).
13. Tenzen, T. *et al.* The cell surface membrane proteins Cdo and Boc are components and targets of the Hedgehog signaling pathway and feedback network in mice. *Dev. Cell* **10,** 647–656 (2006).
14. Chuang, P. T. & McMahon, A. P. Vertebrate Hedgehog signalling modulated by induction of a Hedgehog-binding protein. *Nature* **397,** 617–621 (1999).
15. Seemann, P. *et al.* Activating and deactivating mutations in the receptor interaction site of GDF5 cause symphalangism or brachydactyly type A2. *J. Clin. Invest.* **115,** 2373–2381 (2005).
16. Cheung, M. & Briscoe, J. Neural crest development is regulated by the transcription factor Sox9. *Development* **130,** 5681–5693 (2003).
17. Ericson, J. *et al.* Pax6 controls progenitor cell identity and neuronal fate in response to graded Shh signaling. *Cell* **90,** 169–180 (1997).
18. Lettre, G. *et al.* Identification of ten loci associated with height highlights new biological pathways in human growth. *Nature Genet.* **40,** 584–591 (2008).
19. Weedon, M. N. *et al.* Genome-wide association analysis identifies 20 loci that influence adult height. *Nature Genet.* **40,** 575–583 (2008).

20. Mak, K. K., Chen, M. H., Day, T. F., Chuang, P. T. & Yang, Y. Wnt/β-catenin signaling interacts differentially with Ihh signaling in controlling endochondral bone and synovial joint formation. *Development* **133,** 3695–3707 (2006).
21. Niedermaier, M. *et al.* An inversion involving the mouse Shh locus results in brachydactyly through dysregulation of *Shh* expression. *J. Clin. Invest.* **115,** 900–909 (2005).
22. Sanz-Ezquerro, J. J. & Tickle, C. Fgf signaling controls the number of phalanges and tip formation in developing digits. *Curr. Biol.* **13,** 1830–1836 (2003).
23. Saha, K. & Schaffer, D. V. Signal dynamics in Sonic hedgehog tissue patterning. *Development* **133,** 889–900 (2006).
24. Gong, Y. *et al.* Heterozygous mutations in the gene encoding noggin affect human joint morphogenesis. *Nature Genet.* **21,** 302–304 (1999).
25. Polinkovsky, A. *et al.* Mutations in *CDMP1* cause autosomal dominant brachydactyly type C. *Nature Genet.* **17,** 18–19 (1997).
26. Meyers, E. N., Lewandoski, M. & Martin, G. R. An Fgf8 mutant allelic series generated by Cre- and Flp-mediated recombination. *Nature Genet.* **18,** 136–141 (1998).
27. McLeod, M. J. Differential staining of cartilage and bone in whole mouse fetuses by alcian blue and alizarin red S. *Teratology* **22,** 299–301 (1980).
28. Tsang, K. Y. *et al.* Surviving endoplasmic reticulum stress is coupled to altered chondrocyte differentiation and function. *PLoS Biol.* **5,** e44 (2007).
29. Wai, A. W. *et al.* Disrupted expression of matrix genes in the growth plate of the mouse cartilage matrix deficiency (cmd) mutant. *Dev. Genet.* **22,** 349–358 (1998).

Supplementary Information is linked to the online version of the paper at www.nature.com/nature.

Acknowledgements This work was supported by grants from the Research Grants Council and University Grants Council of Hong Kong (N_HKU705/02, HKU2/02C and AoE/M-04/04), and The National Key Scientific Program (2007CB947300). We thank P. Tam for suggestions and comments, P. Beachy and D. Leahy for sharing unpublished data, and K. Leung for blastocyst injections.

Author Contributions The primary affiliation for J.H. is Bio-X Center, Shanghai Jiao Tong University. B.G. and J.H. designed and performed the experiments and analysed the data. K.F.L. performed the *in vitro* hedgehog signalling assay. F.W., S.S. and S.M. were involved in the *in situ* analysis of digit formation, micromass cultures and revision of the manuscript. M.C. and J.B. assisted in the chick neural tube electroporation experiments. G.M. performed the PTCH1 competitive binding assay. L.H. was involved in experimental design and manuscript revision. K.S.E.C. was involved in experimental design, generation of the BDA1 mouse, data analysis, interpretation and manuscript revision. D.C. coordinated the experimental design, analysed the data, and together with B.G. and J.H. interpreted the results and wrote the manuscript.

Author Information Reprints and permissions information is available at www.nature.com/reprints. Correspondence and requests for materials should be addressed to D.C. (chand@hkusua.hku.hk) or L.H. (helinhelin@gmail.com).

METHODS

Generation of gene-targeted BDA1 mice. A targeting construct containing a 397G > A substitution (p.E95K mutation)[1] was generated in a 6.2-kb Sca-I/Stu-I *Ihh* genomic DNA fragment (gift from A. P. McMahon), together with a *neo* cassette floxed with *loxP* sites inserted in intron 1 (Supplementary Fig. 1a). Gene targeting was performed in L4 embryonic stem cells, derived from 129Sv/ev blastocysts (K. Cheah, unpublished data). G418-resistant clones with the appropriate homologous recombination events were determined from Southern blot analysis of Eco-RI digested DNA, using internal (3′) or external (5′ and 3′) probes (Supplementary Fig. 1a, b). Mouse chimaeras were generated from targeted embryonic stem cells by blastocyst injections[30], and mice heterozygous for the E95K allele were generated from the chimaeras crossed with β-actin Cre mice[26] to remove the neo cassette. C57BL/6 mice heterozygous for an *Ihh*-null allele ($Ihh^{+/-}$) were obtained from A. P. McMahon[10].

Radiological analysis. X-rays were taken using Kodak Diagnostic film Min-R H MRH-1 on a Senograph 600T Senix HF machine (General Electric). Limb bone lengths were measured on the radiographs, and statistical analysis was performed using Student's *t*-test, with a two-tailed $P < 0.05$ taken as statistically significant.

Skeletal staining. E13.5–E18.5 fetuses, newborn and P10 mice were eviscerated, fixed overnight in 95% ethanol, and then transferred sequentially to 100% ethanol and 100% acetone, followed by staining with Alizarin Red S and Alcian Blue[27].

***In situ* hybridization.** *In situ* hybridization on dewaxed sections was performed as previously described[29], using [^{35}S]-UTP- or digoxigenin-labelled ribopobes for *Col10a1* and *Col2a1* (ref. 29), *PTHrP* and *Ppr*[31], *Ihh*[32], *Gli1*, *Gdf5*, *Ptch1* (ref. 33), *Wnt9a* (ref. 34) and *Fgf8* (ref. 35). For whole-mount *in situ* hybridization, anti-digoxigenin antibody conjugated with alkaline phosphatase (Roche) and Boehringer Mannhein purple substrate (Roche) were used to visualize the signal. All markers were analysed on sections from at least three wild-type and mutant mice.

BrdU incorporation. For pulse labelling of fetal mice, pregnant females at a specified gestational stage were injected intraperitoneally with 200 μg of BrdU per gram of body weight and killed after 2 h For pulse-chase labelling, after the initial 2 h incorporation, 6 mg of thymidine (Sigma) was injected to dilute the BrdU, stopping further incorporation[36,37], and the mice were killed 10 h later. BrdU-positive cells were identified by immunostaining using a staining kit (Zymed). Expression of *Col2a1* (*in situ* hybdrization) on a consecutive section was used to determine the region of the chondrogenic condensation, and the number of BrdU-positive cells in the *Col2a1* region was calculated on several sections from five wild-type and five $Ihh^{E95K/E95K}$ mice.

Luciferase hedgehog signalling assay. A hedgehog-signalling reporter cell line was produced in C3H10T1/2 cells stably co-transefected with an 8× GliBS-luc reporter DNA plasmid (gift from P. Beachy), a CMV-lacZ cassette contained in a 3.8 kb Mun-I/Xho-I fragment excised from pcDNA3.1/V5-His/lacZ (Invitrogen), and a 6.0 kb Sal-I and Eco-RI pGK-neo cassette[38] for colony selection. Hedgehog signalling (luciferase activity) was measured as described with modifications[39]. Reporter cells in 24-well plates were cultured in conditioned medium from COS-7 cells stably expressing IHH and IHH(E95K). After 48 h, luciferase activity from the cells was determined using a kit from Promega, normalized to the concentration of wild-type and IHH(E95K), and to cell number using β-galatosidase activity (Luminescent β-galatosidase reporter system 3; BD Biosciences) as an internal control. Statistical analysis was performed using a Student's *t*-test.

Cell-based assay for the binding between PTCH1 and IHH. Binding affinity of the functional N-terminal fragment of IHH (N-IHH) and IHH(E95K) (N-IHH(E95K)) to PTCH1 was evaluated using an established assay[11]. In brief, glutathione *S*-transferase (GST)-tagged N-IHH and N-IHH(E95K) (pGEX-2T vector) expressed in *Escherichia coli* were affinity purified and the GST tag was removed by thrombin digestion. N-IHH proteins were enzymatically labelled using [γ-^{32}P]-ATP at a protein kinase A (PKA) site engineered at the carboxy terminus. Assays were carried out using EcR-CHO cells stably transfected for ecdysone-inducible expression of Ptc-CTD140 (ref. 11). After induction with ponasterone A, 3×10^5 activated cells were incubated with 20 nM of [^{32}P]-N-IHH and different concentrations of unlabelled wild-type N-IHH or N-IHH(E95K) at 4 °C for 2 h. Binding of [^{32}P]-N-IHH in the presence of N-IHH or N-IHH(E95K) was normalized to the total amount of bound [^{32}P]-N-IHH in the absence of competitors set at 100%, and the N-IHH/PTCH1–CTD140 binding affinity determined from a plot of the bound [^{32}P]-N-IHH against an increasing concentration of unlabelled N-IHH and N-IHH(E95K) proteins.

Chick micromass cultures. RCAS(A)-c*IHH* carrying the chicken *IHH* was provided by A. Vortkamp. RCAS(A)-c*IHH*(E95K) was constructed by site-directed mutagenesis (QuikChange kit, Stratagene). Viral supernatant was produced as previously descrived[40]. Chicken micromass cultures[15] were infected with RCAS(A)-*GFP*, RCAS(A)-c*IHH* or RCAS(A)-c*IHH*(E95K). Co-infection of micromass cultures was performed with either RCAS(B)-*GFP* as a control or RCAS(B)-*HIP*. Cultures were incubated for 5–7 days and stained with Alcian blue for cartilaginous condensations or with alkaline phosphatase for differentiated chondrocytes, and quantified using the Zeiss AutMess analytics tool.

Electroporation and expression of genes in the developing chick neural tube. Fertilized white Leghorn eggs were obtained from Tin Hang Technology Limited and incubated in a humidified incubator at 38 °C. Embryos were staged as described previously[41]. *In ovo* electroporation was carried out as described[16]. Expression constructs were generated in the pCAGGS vector[42] for chicken *IHH*, IHH^{E95K} and *HIP1*, then inserted upstream of an internal ribosomal entry site and nuclear localization sequence tagged-GFP. For electroporation, plasmid DNA was injected into the lumen of Hamburger Hamilton stage 11–12 neural tubes. Electroporation was carried out using a BTX electroporator delivering five 50-ms pulses of 30V across the neural tube. Transfected embryos were incubated for 24 h before processing for immunohistochemistry using antibodies for GFP (AB-Direct) and NKX2-2 (DSHB) as described[43]. The monoclonal antibodies against NKX2-2 (74.5A5, developed by T. M. Jessell) were obtained from the Developmental Studies Hybridoma Bank developed under the auspices of the NICHD and maintained by The University of Iowa Department of Biological Sciences.

30. Nagy, A., Gertsenstein, M., Vintersten, K. & Behringer, R. R. *Manipulating the Mouse Embryo. A Laboratory Manual* (Cold Spring Harbour Laboratory Press, 2003).
31. Lee, K. *et al.* Parathyroid hormone-related peptide delays terminal differentiation of chondrocytes during endochondral bone development. *Endocrinology* **137,** 5109–5118 (1996).
32. Bitgood, M. J. & McMahon, A. P. *Hedgehog* and *Bmp* genes are coexpressed at many diverse sites of cell–cell interaction in the mouse embryo. *Dev. Biol.* **172,** 126–138 (1995).
33. Mundlos, S. Skeletal morphogenesis. *Methods Mol. Biol.* **136,** 61–70 (2000).
34. Spater, D. *et al.* Wnt9a signaling is required for joint integrity and regulation of *Ihh* during chondrogenesis. *Development* **133,** 3039–3049 (2006).
35. Crossley, P. H. & Martin, G. R. The mouse *Fgf8* gene encodes a family of polypeptides and is expressed in regions that direct outgrowth and patterning in the developing embryo. *Development* **121,** 439–451 (1995).
36. Haaf, T. High-resolution analysis of DNA replication in released chromatin fibers containing 5-bromodeoxyuridine. *Biotechniques* **21,** 1050–1054 (1996).
37. Schmahl, J., Eicher, E. M., Washburn, L. L. & Capel, B. *Sry* induces cell proliferation in the mouse gonad. *Development* **127,** 65–73 (2000).
38. Adra, C. N., Boer, P. H. & McBurney, M. W. Cloning and expression of the mouse *pgk-1* gene and the nucleotide sequence of its promoter. *Gene* **60,** 65–74 (1987).
39. Taipale, J. *et al.* Effects of oncogenic mutations in *Smoothened* and *Patched* can be reversed by cyclopamine. *Nature* **406,** 1005–1009 (2000).
40. Logan, M. & Tabin, C. Targeted gene misexpression in chick limb buds using avian replication-competent retroviruses. *Methods* **14,** 407–420 (1998).
41. Hamburger, V. & Hamilton, H. L. A series of normal stages in the development of the chick embryo. 1951. *Dev. Dyn.* **195,** 231–272 (1992).
42. Niwa, H., Yamamura, K. & Miyazaki, J. Efficient selection for high-expression transfectants with a novel eukaryotic vector. *Gene* **108,** 193–199 (1991).
43. Briscoe, J., Chen, Y., Jessell, T. M. & Struhl, G. A hedgehog-insensitive form of Patched provides evidence for direct long-range morphogen activity of sonic hedgehog in the neural tube. *Mol. Cell* **7,** 1279–1291 (2001).